Applied Bionics and Biomechanics 9 (2012) 267–274
DOI 10.3233/ABB-2011-0052
IOS Press

Proof of concept: Model based bionic muscle with hyperbolic force-velocity relation

D.F.B. Haeufle[a,b,*], M. Günther[a,c], R. Blickhan[c] and S. Schmitt[a,b]
[a]*Universität Stuttgart, Institut für Sport- und Bewegungswissenschaft, Allmandring, Stuttgart, Germany*
[b]*Universität Stuttgart, Stuttgart Research Centre for Simulation Technology (SRC SimTech), Pfaffenwaldring, Stuttgart, Germany*
[c]*Friedrich-Schiller-Universität, Institut für Sportwissenschaft, Lehrstuhl für Bewegungswissenschaft, Seidelstrasse, Jena, Germany*

Abstract. Recently, the hyperbolic Hill-type force-velocity relation was derived from basic physical components. It was shown that a contractile element CE consisting of a mechanical energy source (active element AE), a parallel damper element (PDE), and a serial element (SE) exhibits operating points with hyperbolic force-velocity dependency. In this paper, a technical proof of this concept was presented. AE and PDE were implemented as electric motors, SE as a mechanical spring. The force-velocity relation of this artificial CE was determined in quick release experiments. The CE exhibited hyperbolic force-velocity dependency. This proof of concept can be seen as a well-founded starting point for the development of Hill-type artificial muscles.

Keywords: Artificial muscle, elastic actuator, Hill relation, quick release, biomechanics, bionics

1. Introduction

Human and animal movement is driven by muscle, a biological elastic actuator. A glance at the complexity and variety of the generated movements shows that muscle is a versatile, powerful, and flexible actuator. This is achieved because muscle can operate in different modes depending on the contraction dynamics and the structural implementation. From a robotics and prosthetics point of view, it would be desirable to have an artificial actuator with similar capabilities.

The contraction dynamics of muscle has been recorded and described in numerous muscle experiments. To interpret the results Hill [12] proposed a macroscopic mathematical model for a contractile element (CE). This CE describes phenomenologically the force-length and the force-velocity dependency of muscle fibers. For the force-velocity relation in concentric contractions (shortening muscle) he found that the muscle fiber shortening velocity depends on the CE force in a hyperbolic relation. This hyperbolic relation is now known as the Hill relation. On the basis of this muscle model a whole class of Hill-type muscle models emerged. These models consist mainly of three elements: CE, serial, and parallel elastic elements in diverse configurations [7, 20, 25, 28, 29]. Various extensions account for physiologically observable effects, such as contraction history effects [15, 19], high frequency oscillation damping [9], and eccentric contractions [22].

In a bionics approach it is an enormous challenge to realize all these properties of biological muscles in one artificial muscle at once. Fortunately, with knowledge about the task specific functional role of these

*Corresponding author: D. Haeufle, Universität Stuttgart, Institut für Sport- und Bewegungswissenschaft, Allmandring 28, D-70569 Stuttgart, Germany. E-mail: daniel.haeufle@inspo.uni-stuttgart.de.

properties it is possible to evaluate their importance. The force-velocity relation e.g. plays a crucial role for the stabilization of human periodic hopping [6, 10] and explosive jumping [25]. A biologically inspired artificial muscle suitable for legged hopping and jumping should therefore feature (hyperbolic) force-velocity characteristics.

Recently Günther & Schmitt [8] analytically derived the hyperbolic Hill-type force velocity relation from basic physical components. They showed that a CE consisting of a mechanical energy source (active element AE), a parallel damper element (PDE), and a serial element (SE) exhibits operating points with hyperbolic force-velocity dependency. In this concept, the force velocity relation is no longer a phenomenological outcome of a black box (i.e. the CE) but rather a physical outcome of the interaction of the three elements AE, PDE, and SE. Therefore, this concept can be interpreted as a basic engineering design for the CE of a Hill-type artificial actuator.

In this paper we present a technical set up to prove the real-world functionality of this concept. With this we want to tackle the gap between macroscopic Hill-type muscle models and engineered actuators in a bionic approach.

2. Methods

The design of the artificial muscle prototype was based on the theory of Günther & Schmitt [8] and the properties of a rat gastrocnemius muscle [26]. To investigate its force-velocity relation quick release experiments were performed.

2.1. Components of the CE

Günther & Schmitt [8] derived a hyperbolic force-velocity relation for the construct drawn schematically in Fig. 2. It consisted of three elements: active element AE, parallel damping element PDE and serial element SE making up together the contractile element CE of a Hill-type muscle. y_0 represented the origin of the muscle, y_1 was the coordinate specifying the length of the AE and the PDE $l_{\mathrm{AE}} = l_{\mathrm{PDE}} = y_1 - y_0$ and y_2 the length of the whole contractile element $l_{CE} = y_2 - y_0$. The forces generated by the elements are in equilibrium:

$$F_{\mathrm{CE}} = F_{\mathrm{SE}} = F_{\mathrm{AE}} + F_{\mathrm{PDE}} \tag{1}$$

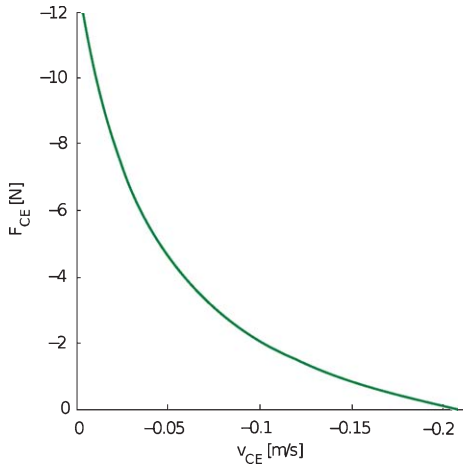

Fig. 1. Force-velocity relation of a rat gastrocnemius muscle as measured by [26] and theoretically predicted by [8].

PDE: Günther & Schmitt [8] specified the functional dependency of the PDE:

$$F_{\mathrm{PDE}} = d_{\mathrm{PDE}} \cdot (\dot{y}_1 - \dot{y}_0) = d_{\mathrm{PDE}} \cdot \dot{l}_{\mathrm{AE}} \tag{2}$$

where $\dot{y}_i = dy_i/dt$. The PDE force depended linearly on the contraction velocity of the AE ($\dot{l}_{\mathrm{AE}}$) with the damping coefficient

$$d_{\mathrm{PDE}}(F_{\mathrm{CE}}) = D_{\mathrm{PDE,max}} \cdot ((1 - R_{\mathrm{PDE}}) \cdot \frac{F_{\mathrm{CE}}}{F_{\mathrm{AE,max}}} + R_{\mathrm{PDE}}) \tag{3}$$

depending linearly on the current force F_{CE} of the CE. $F_{\mathrm{AE,max}}$ was the maximum isometric force, $D_{\mathrm{PDE,max}}$ the maximum $d_{\mathrm{PDE}}(F_{\mathrm{CE}})$ value (at $F_{\mathrm{CE}} = F_{\mathrm{AE,max}}$) and R_{PDE} the minimum $d_{\mathrm{PDE}}(F_{\mathrm{CE}})$ value (passive damping in an inactive muscle) normalized to $D_{\mathrm{PDE,max}}$ [8].

AE: The force produced by the AE is

$$F_{\mathrm{AE}} = A_{\mathrm{AE}} \cdot F_{\mathrm{AE,max}} \tag{4}$$

where the parameter $0 \leq A_{\mathrm{AE}} \leq 1$ allows linear scaling of the AE force. This is taken from biology, where A_{AE} represents the activation state of a muscle [29].

SE: For the SE we chose a mechanical spring which makes the force of the SE

$$F_{\mathrm{SE}} = \begin{cases} -k_{\mathrm{SE}} \cdot \Delta l_{\mathrm{SE}} & \Delta l_{\mathrm{SE}} > 0 \\ 0 & \Delta l_{\mathrm{SE}} \leq 0 \end{cases} \tag{5}$$

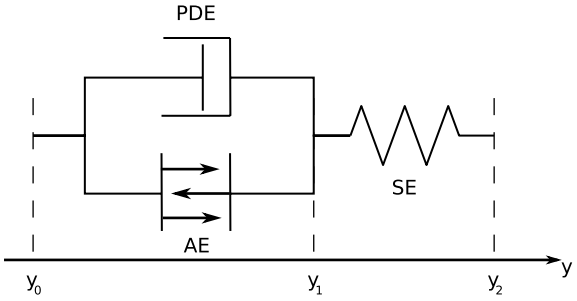

Fig. 2. Theoretical construct of the CE [8]. The CE consists of three elements: Active element AE, parallel damping element PDE, and serial element SE. $y_0 = 0$ is the origin of the CE, y_1 represents the length of the AE/PDE and y_2 the length of the whole CE.

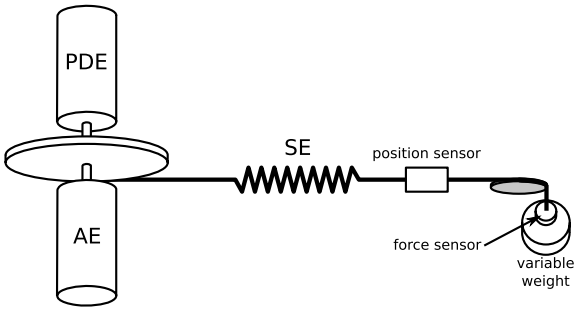

Fig. 3. Hardware design. AE and PDE were realized with electric motors, SE with a mechanical spring. A variable weight was used for the external loading of the CE.

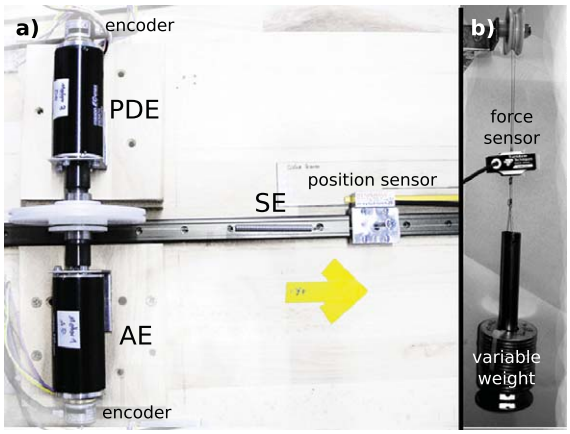

Fig. 4. Picture of the assembly. The components are connected with steel wires. Encoders record the position of the motor shafts (y_1). The position sensors (for y_2) is mounted to a linear guide and attached to the steel wire between spring and force sensor.

where k_{SE} is the spring constant, $\Delta l_{SE} = y_2 - y_1 - l_{SE,0}$, and $l_{SE,0}$ the slack length of the spring.

2.2. Parameter identification

For the elements described above the following Hill-type hyperbolic force-velocity relation

$$(F_{CE} + A) \cdot \dot{l}_{CE} = -B \cdot (F_{CE,0} - F_{CE}) \tag{6}$$

is predicted [8], where the Hill parameters A and B are directly related to the parameters of the three components

$$A = \frac{R_{PDE}}{(1 - R_{PDE}) \cdot (1 - \kappa_v)} \cdot F_{AE,max} + \frac{\kappa_v}{1 - \kappa_v} \cdot F_{CE,0} \tag{7}$$

$$B = \frac{1}{\frac{D_{PDE,max}}{F_{AE,max}} \cdot (1 - R_{PDE}) \cdot (1 - \kappa_v)} \tag{8}$$

with $\kappa_v = (\dot{y}_2 - \dot{y}_1)/\dot{y}_2 = \dot{l}_{SE}/\dot{l}_M$ being the relation between the contraction velocity of the SE and the whole CE.

These relations can be transposed to determine the parameters of the PDE:

$$R_{PDE} = \frac{1}{1 + \frac{F_{AE,max}}{A(1-\kappa_v) - \kappa_v \cdot F_{CE,0}}} \tag{9}$$

$$D_{PDE,max} = \frac{F_{AE,max}}{B(1 - R_{PDE})(1 - \kappa_v)} \tag{10}$$

For a rat GM with $F_{AE,max} = 13.39\,\mathrm{N}$ the constants A and B were experimentally determined to be $A = 2.68\,\mathrm{N}$ and $B = 4.16 \times 10^{-2}\,\mathrm{ms}^{-1}$ ([26], Animal 1). With the assumptions $\kappa_v = 0.15$ and $F_{CE,0} = F_{AE,max}$, the parameters of the PDE result in

$$R_{PDE} = 0.02$$

$$D_{PDE,max} = 386\,\mathrm{Nsm}^{-1}$$

The resulting force-velocity relation is shown in Fig. 1.

2.3. Hardware implementation

AE and PDE: both AE and PDE were realized each with an electric motor (Maxon ECmax40) as shown in Figs. 3 and 4. The motor torque (assuming motor torque is proportional to motor current $T \propto I$) was controlled by Maxon digital EC-motor control units (DEC 70/10).

Both motors were mounted from opposite sites to the same disc with radius $r_{\text{disk}} = 0.05\,\text{m}$. The disc was used to coil up a steel rope and exert a force

$$F_{\text{AE}} + F_{\text{PDE}} = r_{\text{disk}} \cdot (T_{\text{MotorAE}} + T_{\text{MotorPDE}}) \quad (11)$$

on the rope. The force characteristics of the PDE and AE (Equations (2) and (4)) were implemented in Matlab Simulink through Real Time Workshop and Real Time Windows Target. In this way the motors could exert the specified force on the steel rope and the SE as required by the theoretical construct. This was validated for the torques and speeds occurring during the experiments (current controller bandwidth $\approx 1\,\text{kHz}$, motor included >100 Hz, peak target frequencies $\approx 30\,\text{Hz}$).

SE: either a soft spring (spring constant $k_{\text{SE}} = 369\,\text{Nm}^{-1}$), or a stiff spring ($k_{\text{SE}} = 2401\,\text{Nm}^{-1}$) was tight on one end to the steel rope of the motor disc and on the other end to a variable weight (Fig. 3).

Sensors: the motor shaft position φ_{Motor} was recorded by an optical encoder (Scancon 2RMHF 5000 pulses/revolution) and represented $y_1 = 2r_{\text{disk}}\varphi_{\text{Motor}}$. An optical linear position encoder (Renishaw RGH24D 5 μm resolution) recorded y_2. A load cell (Transducer Techniques MLP 25 with amplifier TM0-1-24) recorded the force F_{CE}. All sensor data was recorded with Matlab Simulink via a Sensoray 626 AD I/O at 1 kHz.

Test-bed: the motors were mounted to a table (at y_0). A variable weight was attached to the SE via a wheel at the end of the table. An electromagnet was installed below the weight to restrain the movement of the weight for isometric and quick release experiments.

2.4. Measurement protocol

To investigate the force-velocity characteristics of the artificial CE two types of experiments had to be performed. The first experiment was an **isometric contraction** (contraction with constant CE length: $y_2 - y_0 = \text{const.}$). Hereto the weight was fixed with the electromagnet guaranteeing a constant CE length. Then the AE activation was set to $A_{\text{AE}} = 1$ (maximum activation) and the shortening of the AE (rotation of the motors) was recorded. The time from the beginning of the activation until the end of AE shortening t_{isom} and the maximum isometric force $F_{\text{CE}}(t_{\text{isom}}) = F_{\text{CE,max}}$ were evaluated.

The **quick release contraction** experiments started like an isometric contraction. Only that the weight was released at $t_{\text{QR}} > t_{\text{isom}}$ (soft spring: $t_{\text{QR}} = 8\,\text{s}$, stiff spring: $t_{\text{QR}} = 3\,\text{s}$). The recorded CE contraction velocity $v_{\text{CE}} = \dot{y}_2$ (example in Fig. 5a and b) shows a global minimum shortly after t_{QR} at $t_{v\text{CE\_min}}$. The values $v_{\text{CE}}(t_{v\text{CE\_min}})$ and $F_{\text{CE}}(t_{v\text{CE\_min}})$ were extracted. This experiment was performed with different weights $0.2\,\text{kg} \leq m \leq F_{\text{CE,max}}/9.81\,\text{ms}^{-2}$ in steps of $\approx 0.08\,\text{kg}$, five times per weight. The curve $F_{\text{CE}}(t_{v\text{CE\_min}})$ vs. $v_{\text{CE}}(t_{v\text{CE\_min}})$ for all weights represents the force-velocity characteristics of the artificial CE (Fig. 5c and d).

3. Results

The force-velocity relation of the artificial CE is shown in Fig. 5 for the soft c) and the stiff d) SE. A hyperbola (Equation (6)) was fitted to the data. The coefficients of the fit are listed in Table 1. For the soft spring the fit is better for lower than for higher velocities. For the stiff spring the fit maps the experimental results quite well, however, it cannot capture the effects around $v_{\text{CE}} = -0.1\,\text{ms}^{-1}$. The measurements result in reproducible clusters of five data points for each load. The ratio between SE and CE contraction velocity $\kappa_v(t) = (v_{\text{CE}}(t) - v_{\text{AE}}(t))/v_{\text{CE}}(t)$ was also extracted for $t = t_{v\text{CE\_min}}$ (Fig. 5e and f). Measured values for κ_v mostly deviate from the assumption of $\kappa_v = 0.15$.

4. Discussion

We could reproduce a Hill-type hyperbolic force-velocity relation in an artificial muscle prototype. The prototype was based on a theoretical model which describes the assembly of three basic physical components: AE, PDE, and SE [8]. Although this model analytically predicts operating points on a hyperbolic force-velocity relation it cannot predict the time-dependency of the contraction dynamics. Still, the force-velocity relation of the prototype is qualitatively hyperbolic, but quantitatively deviates from the prediction (Fig. 5c and d). With the prototype showing a hyperbolic force-velocity relation in quick release contractions, we were able to proof the real-world functionality of this concept.

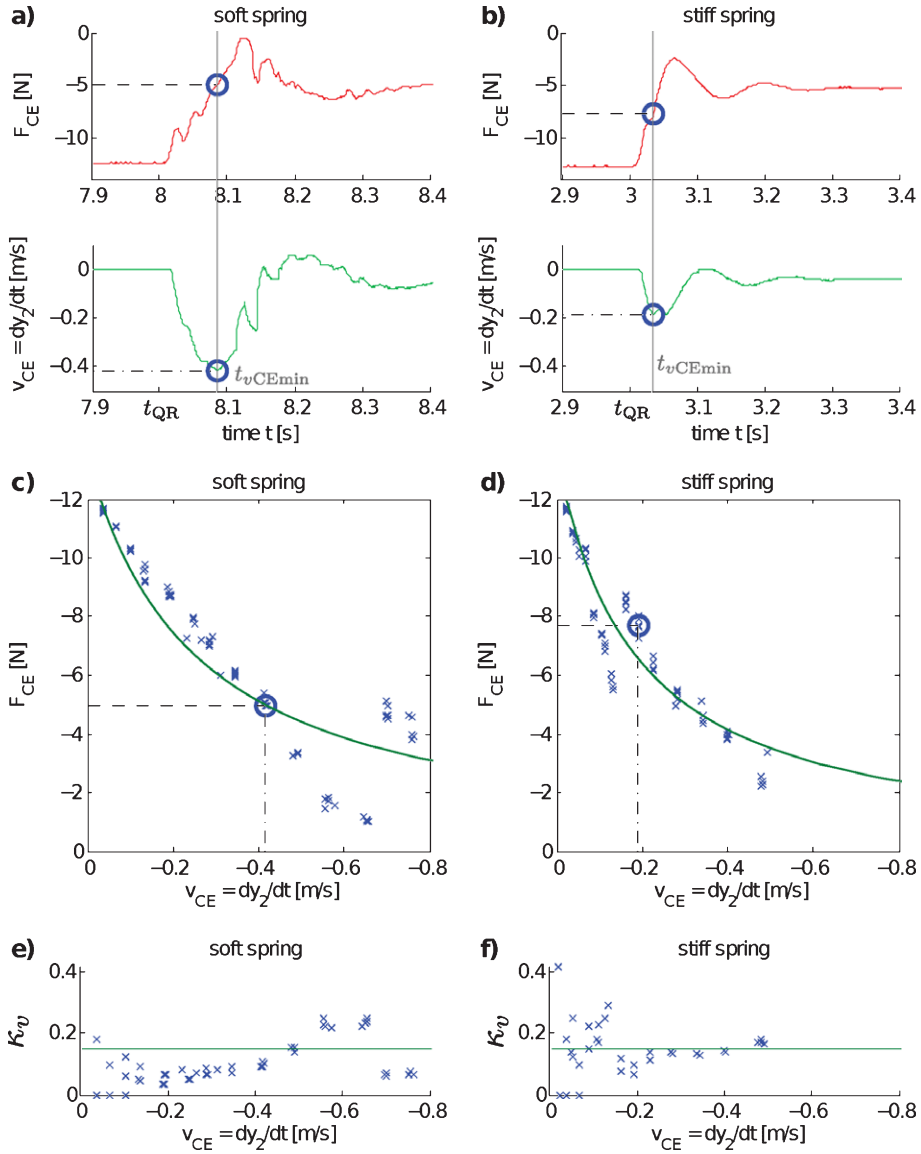

Fig. 5. QR results with SE soft spring ($k_{SE} = 369\,\mathrm{Nm}^{-1}$) and SE stiff spring ($k_{SE} = 2401\,\mathrm{Nm}^{-1}$). a) and b): Force and contraction velocity of the CE during a quick release experiment (QR load: $m = 0.523\,\mathrm{kg}$). The load was released at t_{QR}. The contraction velocity v_{CE} reached a minimum at t_{vCE_min} (circle). $F_{CE}(t_{vCE\_min})$ and $v_{CE}(t_{vCE\_min})$ were extracted. c) and d): Force velocity relation $F_{CE}(t_{vCE\_min})$ vs. $v_{CE}(t_{vCE\_min})$ derived from QR experiments. The circle refers to the QR experiment shown in Fig. a) and b). A hyperbola was fitted to the data (fit parameters see table 1). It deviates from the theoretical prediction (Fig. 1). e) and f): actual (x-marks) and assumed (solid line) ratio between SE and CE contraction velocity $\kappa_v(t) = (v_{CE}(t) - v_{AE}(t))/v_{CE}(t)$ for $t = t_{vCE\_min}$.

Table 1
Hyperbola fit coefficients for the equation $(F_{CE} + A) \cdot \dot{l}_{CE} = -B \cdot (F_{CE,0} - F_{CE})$

Force-velocity relation of	A [N]	B [ms^{-1}]	$F_{CE,0}$ [N]	r^2
Rat GM from measurements ([26] Animal) and analytical prediction by the model of Günther & Schmitt [8]	2.68	0.04	13.39	N/A
Artificial CE with SE soft spring	0.24	0.26	13.39	0.86
Artificial CE with SE stiff spring	0.20	0.19	13.39	0.88

r^2 is given as a measure for the quality of the fit.

4.1. Meaning of the parameters

In the current state of model development [8] κ_v can be chosen as a free parameter. Here, we used $\kappa_v = 0.15$ and calculated the parameters for the PDE. The resulting experimental κ_v deviates from this assumption (Fig. 5e and f). Therefore, the force-velocity relations (Fig. 5c and d) deviate from the theoretical expectation (Fig. 1) too. This affirms that there is some indeterminacy and redundancy in the model so far because κ_v itself is a free parameter. For the model limit case $R_{\mathrm{PDE}} \to 0$ (which is just 2% here) e.g., calculations result in $A_{\mathrm{rel}} = \kappa_v/(1-\kappa_v) = A/F_{\mathrm{CE},0} = 2.68\,\mathrm{N}/13.39\,\mathrm{N} = 0.2$ which gives $\kappa_v = 0.25$. We therefore see κ_v ready to be fitted to experimental A and B values or to be derived from further model assumptions as, e.g. parametrizing AE and SE.

Beyond the model [8] we now introduced the simplest possible concrete hardware implementation of the SE characterized by the stiffness parameter k_{SE}. At first sight, κ_v now seems to be a parameter to be predicted by the model itself rather than to be fitted from experimental A,B combinations. This is as two elements in series (PDE and SE) are now parametrized and force equilibrium and kinematic coupling might appear to be sufficient for prediction ([8], see appendix). For the AE, other properties like length dependencies are not substantiated beyond its current (constant) force value F_{AE}. Thus, both the theoretical model in its current state [8] and our presented hardware implementation are still deficient in a sense that they can not uniquely self-predict κ_v values, i.e. derive it from all other parameters.

Our hardware implementation of the model is straight forward, i.e. the implementation directly maps all elements as formulated by Günther & Schmitt [8], but further substantiates the element SE by a serial spring with a specific stiffness. Measured κ_v values apparently do not depend on SE stiffness. This is somehow surprising because the stiffer the serial spring is the lower its contribution to CE contraction (decreasing κ_v) would be expected. From this and the above explained indeterminacy of the model, we conclude that the muscle model [8] itself must be scrutinized again. Current indeterminacy and seeming contrariness between biological muscle, muscle model and our hardware implementation are, however, not detrimental to the fact that our simple and transparent implementation of an artificial muscle based on a blueprint directly taken from a very reduced muscle model proved that the model concept works in real world.

4.2. The force-velocity relation

The force-velocity relation is an outstanding dynamic property of biological muscles. It can be observed in muscles of insects [1], spiders [21], frogs [12], mammals [9, 26] and other animals. The relation between force and velocity was always found to be of hyperbolic nature.

The strength of Hill's [12] approach is that only three parameters are necessary to describe the observed force-velocity characteristics during concentric contractions: the Hill-parameters A and B and the isometric muscle force $F_{\mathrm{M},0}$. These parameters can be determined in: 1) Quick release experiments: peak shortening velocity is measured in contractions against a constant load, as described in this paper (see also e.g. [9, 14, 17]). 2) isokinetic contractions: the force is measured for constant contraction velocities. The second method was used by van Zandwijk et al. [26] to determine the Hill-parameters for rat gastrocnemius muscles which were used as a reference in this paper. Ettema & Huijing [3] showed that both experiments give the same results.

One benefit of the force-velocity relation is the counteraction to movement perturbations. In simulation studies it was shown that the first mechanical reaction of muscles (preflex) to arm movement perturbations is mainly determined by the force-velocity relation which generates a strong restoring force [2]. Furthermore, with force-velocity relation muscles can stabilize periodic movements, like hopping [6, 10, 27]. Although this can be achieved already with a linear approximation to the force-velocity relation, the hyperbolic relation results in a faster reduction of perturbations [10].

The theory predicts a hyperbolic force-velocity relation for our artificial CE (Fig. 1). The experimental data can be fitted with a hyperbola – a linear fit explained the experimental data rather worse (soft spring: $r^2 = 0.80$ and stiff spring $r^2 = 0.84$) – but high frequency oscillations during the quick-release contraction (Fig. 5a and b) cause the observed scattering (Fig. 5c and d). These high frequency oscillations could be reduced by incorporating a small damping in the SE [9]. That this would most likely result in a smoother hyperbola can be seen when filtering force and velocity data (Fig. 6).

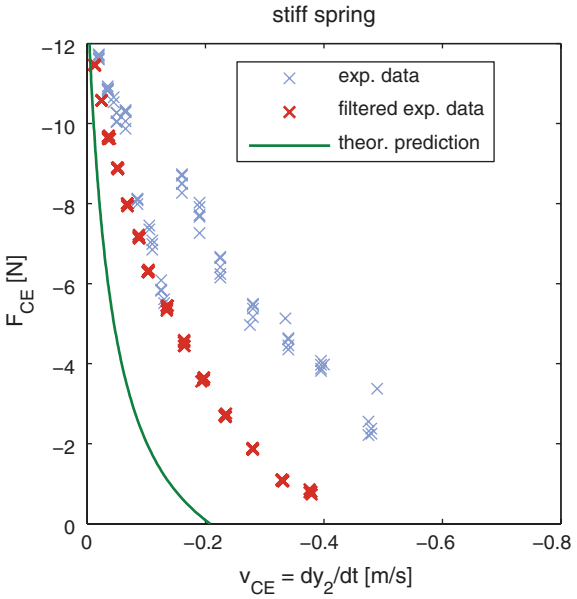

Fig. 6. Comparison of raw experimental data (faint blue x's) filtered experimental data (dark red x's) and theoretical prediction (green line). The experimental force and velocity data was filtered with a 4th order Butterworth low-pass filter at a cutoff frequency $f = \frac{1}{2\pi}\sqrt{k/m}$. (Colours are visible in the online version of the article; http://dx.doi.org/10.3233/ABB-2011-0052)

A remark on the force-length relation and the activation level – also important characteristics of biological muscle – which were neglected in the current prototype: here, we purely aimed to proof, that a hyperbolic force-velocity relation emerges from the embodyment of the three mechanical elements AE, PDE, and SE. In the future development of an artificial muscle, they will have to be incorporated.

4.3. Artificial muscles

Generally, an improvement in performance of technical systems, e.g. robot arms, walking machines and prostheses, from actuators incorporating muscle-like characteristics are expected. Therefore, a broad variety of such technical actuators were developed in the past.

Electric drives can be coupled with spring elements to generate compliant characteristics [18]. Hereby, the torque-rotation speed characteristics can be seen as an equivalent to the force-velocity relation of real muscles. In particular, electro-magnetic and electromechanical actuators show hyperbolic torque-rotation speed characteristics [5]. However, to achieve torque and velocity values needed to drive walking machines or robots, fast rotating electric motors have to be combined with gear boxes. Friction and inertial forces of the used gears hinder muscle-like performance in the end.

Other muscle-like actuators showing a hyperbolic force-velocity relation and incorporating compliance are known [11]. However, those actuators lack scalability and the possibility to adapt muscle characteristics dynamically. In detail, they presume the requested force and individually modify a strain rate in series to the motor.

Material-dependent compliance and damping can be produced by the use of elastomers as technical actuators [16]. But neither compliance nor damping values of such elastomers are comparable to those needed to produce muscle-like characteristics. Particularly, the damping coefficient is inversely hyperbolic (in contrast to biological muscles it is increasing with increasing contraction velocity) and in general too low for low contraction velocities [16].

Pneumatic artificial muscles, also known as "Mc Kibben muscles", e.g. FESTO fluidic muscle [4], show a force-velocity relation of hyperbolic nature [13, 23, 24]. However, structural problems of the "McKibben" technology remain: inconstant volumes during contractions, significant hysteresis already at very low contractions velocities, smaller shortening rates than real muscles, energetically less efficient than other technical actuators, and they need an air compressor.

The proof of concept of an artificial muscle presented here is based only on a very small number of mechanical elements and an inherently simple control algorithm. Still, it shows already the contraction characteristics of real biological muscle with the incorporation of high robustness and self-stability. Altogether, with this actuator it is possible to produce movement characteristics similar to that of real biological muscle on the level of movement, generation.

Acknowledgments

We would like to mention that an earlier version of this Paper appears in the proceedings of the 1st International Conference on Applied Bionics and Biomechanics (ICABB), held in Venice, Italy, on October 14–16, 2010. Also, we would like to acknowledge that this work was supported by a Research Seed Capital (RisSC) — Tranche 2009 from the Ministry of

Science, Research and Arts of Baden-Württemberg and the University of Stuttgart (Kapitel 1403 Tit.Gr. 74). We also like to thank Brian Kaluf for contributing to our first steps in the project and Per Schmitt and Edgar Schmitt for their technical support.

References

[1] A.N. Ahn and R.J. Full, A motor and a brake: Two leg extensor muscles acting at the same joint manage energy differently in a running insect, *Journal of Experimental Biology* **205**(3) (2002), 379–389.

[2] I.E. Brown and G.E. Loeb, A reductionist approach to creating and using neu-romusculoskeletal models, *Biomechanics and Neural Control of Posture and Movement* (2000), 148–163.

[3] G.C. Ettema and P.A. Huijing, Isokinetic and isotonic force-velocity characteristics of rat EDL at muscle optimum length, G. De Groot, A.P. Hollander, P.A. Huijing and G.J. Van Ingen Schenau, (eds), *Biomechanics XI-A, International Series on Biomechanics 7-A*, Free University Press, Amsterdam, (1988), 58–62.

[4] FESTO AG. & Co., *Pneumatische Federelementanordnung insbesondere zur Niveaureg-ulierung von Kraftfahrzeugen*. Tech. rept. DE 100 52 663 Cl, 2000.

[5] T. Frank and C. Schilling, The development of cascadable microdrives with muscle-like operating behaviour, *Journal of Micromechanics and Microengineering* **8** (1998), 222.

[6] H. Geyer, A. Seyfarth and R. Blickhan, Positive force feedback in bouncing gaits? *Proceedings of the Royal Society of London, Series B* **270**(1529) (2003), 2173–2183.

[7] M. Günther and H. Ruder, Synthesis of two-dimensional human walking: A test of the lambda-model, *Biological Cybernetics* **89**(2) (2003), 89–106.

[8] M. Günther and S. Schmitt, A macroscopic ansatz to deduce the Hill relation, *Journal of Theoretical Biology* **263**(4) (2010), 407–418.

[9] M. Günther, S. Schmitt and V. Wank, High-frequency oscillations as a consequence of neglected serial damping in Hill-type muscle models, *Biological Cybernetics* **97**(1) (2007), 63–79.

[10] D.F.B. Haeufle, S. Grimmer and A. Seyfarth, The role of intrinsic muscle properties for stable hopping - stability is achieved by the force-velocity relation. *Bioinspiration and Biomimetics* **5**(1) (2010), 016004.

[11] B. Hannaford, K. Jaax and G. Klute, Bio-inspired actuation and sensing, *Autonomous Robots* **11**(3) (2001), 267–272.

[12] A.V. Hill, The heat of shortening and the dynamic constants of muscle, *Proceedings of the Royal Society of London, Series B* **126**(843) (1938), 136–195.

[13] T. Kerscher, J. Albiez, M. Zollner and R. Dillmann, Evaluation of the dynamic modeling of fluidic muscles using quick-release, *Proceedings of the first IEEE/RAS-EMBS International Conference on Biomedical Robotics and Biomechatronics* (2006), 637–642.

[14] T.A. McMahon, *Muscles, reflexes and Locomotion*, Princeton University Press, (1984).

[15] K. Meijer, H.J. Grootenboer, H.F.J.M. Koopman, B.J.J.J. van Der Linden and P.A. Hui-jing, A Hill type model of rat medial gastrocnemius muscle that accounts for shortening history effects, *Journal of Biomechanics* **31**(6) (1998), 555–563.

[16] R. Pelrine, R. Kornbluh, Q. Pei, S. Stanford, S. Oh, J. Eckerle, R.J. Full, M.A. Rosenthal and K. Meijer, Dielectric elastomer artificial muscle actuators: Toward biomimetic motion, *Proceedings of SPIE*. SPIE-International Society for Optical Engineering. **4695**(2002), 126–137.

[17] C.A.K. Phillips, J. Richard and E. Crouch, Velocity of mammalian skeletal muscle contraction as a function of fiber type, activation, initial length and temperature, *Computers in Biology and Medicine* **22**(4) (1992), 247–262.

[18] G.A. Pratt and M.M. Williamson, Series elastic actuators, *Proceedings 1995 IEEE/RSJ International Conference on Intelligent Robots and Systems. Human Robot Interaction and Cooperative Robots* (1995), 399–406.

[19] C. Rode, T. Siebert and R. Blickhan, Titin-induced force enhancement and force depression: A 'sticky-spring' mechanism in muscle contractions? *Journal of Theoretical Biology* **259**(2) (2009), 350–360.

[20] T. Siebert, C. Rode, W. Herzog, O. Till and R. Blickhan, Nonlinearities make a difference: Comparison of two common Hill-type models with real muscle, *Biological Cybernetics* **98**(2) (2008), 133–143.

[21] T. Siebert, T. Weihmann, C. Rode and R. Blickhan, Cupiennius salei: Biomechanical properties of the tibia-metatarsus joint and its flexing muscles, *Journal of Cmparative Physiology B, Biochemical, Systemic and Environmental Physiology* **180**(2) (2010), 199–209.

[22] O. Till, T. Siebert, C. Rode and R. Blickhan, Characterization of isovelocity extension of activated muscle: A Hill-type model for eccentric contractions and a method for parameter determination, *Journal of Theoretical Biology* **255**(2) (2008), 176–187.

[23] B. Tondu, *Artificial Muscles for Humanoid Robots*, I-Tech Education and Publishing, Wien, (2007).

[24] B. Tondu and P. Lopez, Modeling and control of McKibben artificial muscle robot actuators, *IEEE Control Systems Magazine* **20**(2) (2000), 15–38.

[25] A.J. van Soest and M.F. Bobbert, The contribution of muscle properties in the control of explosive movements, *Biological Cybernetics* **69**(3) (1993), 195–204.

[26] J.P. van Zandwijk, M.F. Bobbert, G.C. Baan and P.A. Huijing, From twitch to tetanus: Performance of excitation dynamics optimized for a twitch in predicting tetanic muscle forces, *Biological Cybernetics* **75**(5) (1996), 409–417.

[27] H. Wagner and R. Blickhan, Stabilizing function of skeletal muscles: An analytical investigation, *Journal of Theoretical Biology* **199**(2) (1999), 163–179.

[28] J.M. Winters, *Multiple muscle systems: Biomechanics and movement organization*, Springer-Verlag Berlin and Heidelberg GmbH & Co. Kg. Chap. Hill-based muscle models: A systems engineering perspective (1990), 69–93.

[29] F.E. Zajac, Muscle and tendon: Properties, models, scaling, and application to biome-chanics and motor control, *Critical Reviews in Biomedical Engineering* **17**(4) (1989), 359–411.